*Journal of Physiology* (1990) **422**, *pp.* 351–367
*With 7 figures*
*Printed in Great Britain*



# PROPERTIES OF ENZYMATICALLY ISOLATED SKELETAL FIBRES FROM MICE WITH MUSCULAR DYSTROPHY

BY STEWART I. HEAD, D. GEORGE STEPHENSON AND DAVID A. WILLIAMS*

*From the Department of Zoology, La Trobe University, Bundoora, Victoria 3083, and the * Department of Physiology, University of Melbourne, Parkville, Victoria 3052 Australia*

(*Received 31 March 1989*)

SUMMARY

1. Single intact muscle fibres were enzymatically isolated from the skeletal muscles of the dystrophic mouse 129/ReJ dy/dy and were subjected to a range of physiological interventions.

2. Electrophysiological measurements, diffusion of injected dyes (Lucifer Yellow), microdissection and general appearance in the light microscope have shown that the majority of skeletal fibres isolated from the soleus and extensor digitorum longus (EDL) of adult dystrophic mice (10–14 weeks old) had gross morphological abnormalities. These abnormalities ranged from simple branching of the fibre to interconnections of many fibre branches which form a complex syncitium.

3. Segments from fibres of normal appearance and from fibres with morphological deformities were chemically skinned with Triton X-100 and activated in $Ca^{2+}$- and $Sr^{2+}$-buffered solutions. The different characteristics of the $Ca^{2+}$- and $Sr^{2+}$-activation curves were also used to identify the fibre type.

4. Gross morphological abnormalities were observed both in fibres which had predominantly slow-twitch and fast-twitch characteristics.

5. A new group of fibres was found to exist in the soleus muscle of dystrophic animals and represented about 18% of the entire soleus fibre population. This group of fibres had predominantly fast-twitch characteristics and some of these fibres were also grossly malformed.

6. The activation characteristics of individual branches from the same complex syncitium were similar, indicating that the contractile and regulatory proteins were of one type in one syncitium.

7. Chemically skinned segments from malformed fibres which included a major deformity between the points of attachment were generally unable to sustain near-maximal forces.

8. The proportion of malformed fibres which remained intact decreased markedly after prolonged tetanical stimulation of the intact muscle. This strongly suggests that malformed fibres are also functionally weak and prone to progressive damage when stimulated within the intact muscle.

9. The presence in large proportions of fibres with gross morphological ab-

normalities may explain the symptoms of severe and progressive muscle weakness and muscle loss which are apparent in the 129/ReJ dy/dy mice and possibly even in the human dystrophies such as Duchenne muscular dystrophy.

## INTRODUCTION

The autosomal murine mutant *Dystrophia muscularis* 129/ReJ dy/dy is a commonly used animal model for the muscular dystrophies which displays most of the clinical symptoms of Duchenne muscular dystrophy. The three fundamental characteristics it shares with Duchenne muscular dystrophy – progressive and severe muscle weakness, progressive degeneration and disappearance of skeletal muscle and increased serum activity of sarcoplasmic enzymes (Rowland, 1985) – suggest that a closer study of the disease etiology in this animal model could provide further information relating to the causes of cell damage which occurs in those fibres preferentially affected by Duchenne muscular dystrophy (e.g. fast-twitch fibres; Webster, Silberstein, Hays & Blau, 1988). There have been a number of reports of muscle fibres with structural abnormalities in skeletal muscles from dystrophic 129/ReJ dy/dy mice (Isaacs, Bradley & Henderson, 1973; Harris & Ribchester, 1979; Ontell, Hughes & Bourke, 1982). However, most of these investigations have depended on serial reconstructions of histological sections of the afflicted muscles or the dissection of gluteraldehyde-fixed muscle specimens to obtain information about the structural complexities, and as such the functional significance of these fibres could not be determined.

It was therefore our general aim to develop a method for the isolation of the entire population of single muscle fibres from the skeletal muscles of the dystrophic mouse 129/ReJ dy/dy to enable us to study the properties of fibres with different morphologies. By doing so we hoped to be able to determine whether there may be a causal relationship between the presence and properties of the abnormal fibres and the symptoms (muscle weakness and wastage) of this dystrophy. Preliminary accounts of this work have already appeared (Head, Williams & Stephenson, 1988; Williams, Head, Stephenson & Stephenson, 1988).

## METHODS

*Muscle preparations.* These experiments utilized the extensor digitorum longus (EDL) and flexor digitorum brevis (FDB), both predominantly fast-twitch, and soleus (mixed slow- and fast-twitch) muscles, of phenotypically normal (+/?) and dystrophic (129/ReJ dy/dy) mice. All animals were aged between 10 and 14 weeks and were killed by cervical dislocation.

*Isolation of single muscle fibres.* A number of different enzyme mixtures were utilized to dissociate single intact fibres from the skeletal muscles of normal (+/?) and dystrophic (dy/dy) 129/ReJ mice. These included various combinations of collagenases (Sigma types I or IV), elastase (I), hyaluronidase (I), protease (VII) and trypsin (II). The simplest combination which resulted in greatest digest success (as judged from the percentage yield of viable intact fibres) was either type I collagenase in association with soybean trypsin inhibitor or type IV collagenase alone. This dissociation method is similar to one employed with rat skeletal muscle (Bekoff & Betz, 1977). Intact soleus and EDL muscles were carefully ablated and incubated (37 °C, 2–4 h with constant agitation) in Tyrode solution (mM): 2·5 $Ca^{2+}$, 11·0 glucose, 135 NaCl, 4 KCl, 1 $MgCl_2$, 0·33 $NaH_2PO_4$, 10 HEPES, pH 7·3 with 0·15–0·3 % collagenase (Sigma type IV). The muscle mass was then removed from the incubation mixture and suspended in Tyrode solution, or a relaxing solution (solution A see below). Intact skeletal muscle fibres were separated from the muscle mass

by gently swirling the mixture. A combination of penicillin G, streptomycin sulphate and bovine serum albumin was then added to the cell suspension which was maintained at 5 °C until required for experiments.

*Skinned muscle preparations.* For analysis of the properties of the contractile and regulatory proteins of dystrophic and normal muscle, skeletal muscle fibres were first exposed to a $Na^+$-based relaxing solution (see below). Various fibre segments were then individually clamped at one end in a pair of fine stainless-steel Barcroft forceps (A. Heiss) while the other end was tied with 9·0 braided silk (Deknatel) to an AE875 strain-gauge force transducer (AME, Horten, Norway) as shown diagrammatically in Fig. 7*B* and *D* and described earlier (Fink, Stephenson & Williams, 1986). The sarcolemmal barrier was removed by exposure to 2% Triton X-100 in a $K^+$-based relaxing solution (solution A, see below) for 10 min. The average sarcomere length, measured by laser diffraction as previously described (Stephenson & Williams, 1981), was adjusted in the range 2·60–2·70 $\mu$m. Activation of fibres employed the three solution types (A, B and H) routinely employed in this laboratory which each contained (mM): 117 $K^+$, 36 $Na^+$, 1 $Mg^{2+}$, 60 HEPES, 8 total adenosine 5′-trisphosphate (ATP); 10 creatine phosphate; with 15 U $ml^{-1}$ creatine phosphokinase; the pH was 7·10. In addition the solutions contained either 50 mM-$EGTA^{2-}$ (ethyleneglycol-bis-($\beta$-aminoethylether) *N,N,N′,N′* tetraacetate ions) (solution A), 49–49·5 mM-Ca-$EGTA^{2-}$ and slight excess $EGTA^{2-}$ (0·5–1 mM) (solution B), or 50 mM-HDTA (hexamethylenediamine-*N,N,N′,N′*-tetraacetate ions) (solution H) (Stephenson & Williams, 1981; Fink *et al.* 1986). In $Na^+$-based solutions all $K^+$ was isotonically replaced by $Na^+$. All solutions were designed for use at room temperature (20–25 °C) with the affinity constants previously determined for these experimental conditions (Stephenson & Williams, 1981).

*Stimulation of intact muscle preparations.* A protocol was devised to severely stimulate intact muscles for prolonged periods in an effort to establish whether any fibre population was more susceptible to damage during vigorous contraction, and to determine if irreversible force loss occurred as a result of fibre damage. Intact EDL and soleus muscles ablated from one hindlimb of the dystrophic mouse were attached to a force transducer and repeatedly, tetanically stimulated with field electrodes placed on each side of the muscle (field strength 53 V $cm^{-1}$, $0{\cdot}5^{-1}$ ms duration pulses at 100 Hz). The period of stimulation (10 s, on, 10 s off in blocks of 10 mins) lasted for up to 3 h with short periods of interruption between blocks, after which the muscles were left to recover for 30 min before measurement of the tetanic force response. The contralateral muscles from each animal remained unstimulated and served as a control for the stimulated muscle. Muscles from phenotypically normal mice were also subjected to the same stimulus protocol and served as another control.

*Assessing single fibre boundaries.* The extent of intracellular continuity and fibre viability was determined by loading single intact fibres with the fluorescent dye Lucifer Yellow (lithium salt) by ionophoresis from a single microelectrode (Stewart, 1981). The pulse protocol for loading involved delivery of 6–9 nA negative current pulses (1 s on, 1 s off) for a total of 5–15 min and was precisely controlled with a Model D100 Digitimer (Digitimer Ltd, England). In these fibres resting membrane potential was monitored with the same microelectrode, which could also be used to deliver short depolarizing pulses (5 ms, less than 9 nA) to initiate fibre contraction. Each contraction was monitored by recording video images, captured with a silicon-intensified-target (SIT) camera, on videotape. These images were then analysed frame-by-frame employing a super B video recorder (Sony) with frame-stepping circuitry. Video images of injected cells were digitized directly or from videotape with an 100 Series Image processing board (Imaging Technology, Dindima, Australia) resident in an Olivetti M280 personal computer. Fluorescence images were frame averaged (four to sixteen frames), corrected for illumination inhomogeneities, and then contrast enhanced.

## RESULTS

### *Morphology of isolated muscle fibres*

The yield of fibres generally ranged from 70 to 100% of total fibres present in the intact muscle. These estimates were based on the amount of fibre debris in the dispersal medium at the end of the dissociation procedure. The presence of elastase or hyaluronidase in addition to collagenase had no apparent effect on fibre yields,

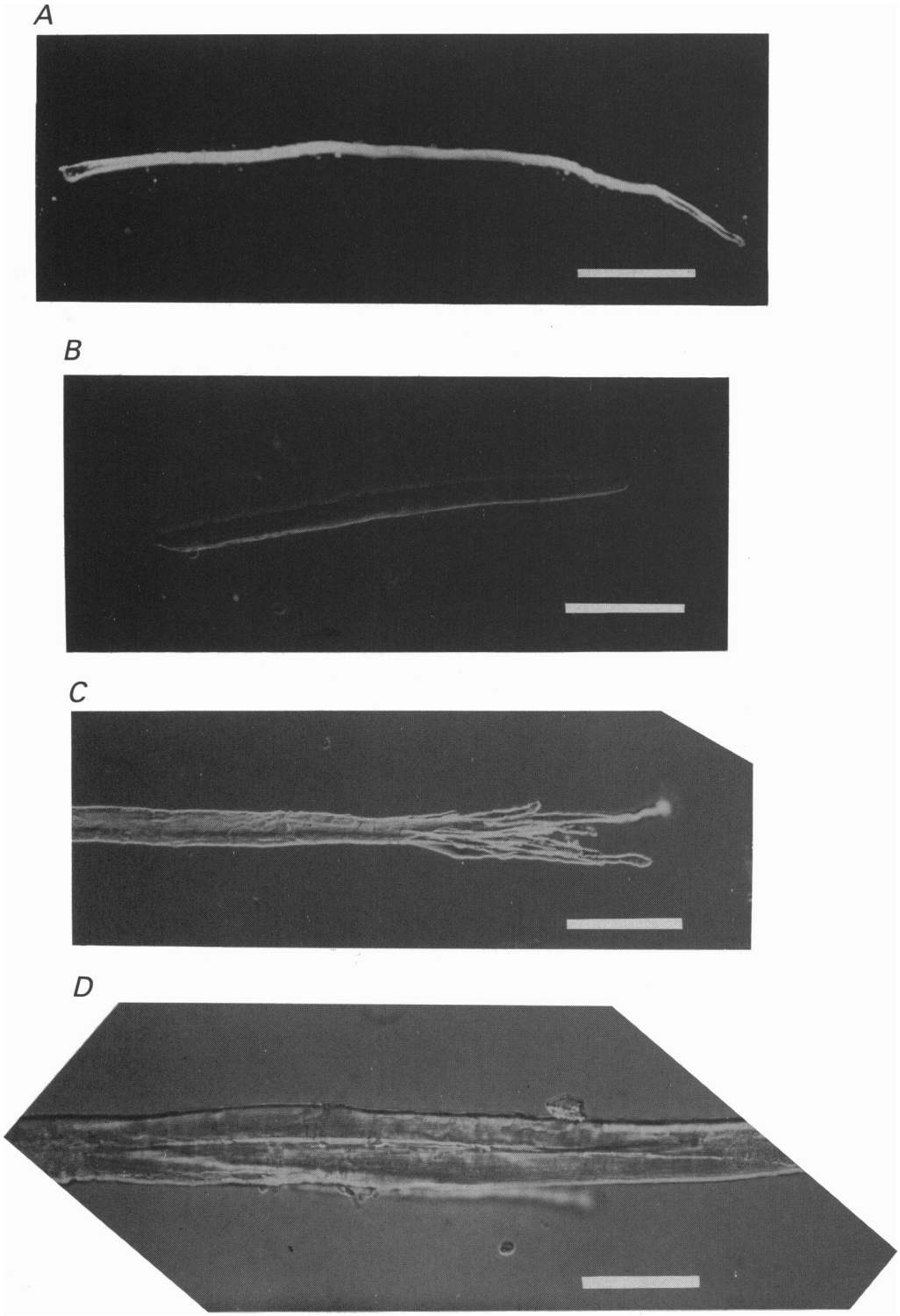


Fig. 1. For legend see facing page.

while trypsin and protease had deleterious effects in that yields were reduced markedly (to 10–15%) and many fibres were damaged or supercontracted.

The dissociation technique liberated individual fibres from muscles of phenotypically normal mice (+/?) which were elongated and gradually tapered at both ends (Fig. 1*A*) and had peripheral nuclei. The fibres isolated from the FDB were generally shorter, rarely exceeding 1 mm, than those of the soleus or EDL which ranged between 0·7 and 15 mm. Fibre diameters in phenotypically normal mice (+/?) ranged between 20 and 60 $\mu$m in all muscles. Less than 50% of fibres from the muscles of dystrophic animals displayed this morphology (Fig. 1*B*). These fibres, in all respects, were visibly indistinguishable from normal fibres (cf. panels *A* and *B* of Fig. 1). In contrast, the majority of single fibres isolated from the muscles of dystrophic animals displayed distinct morphological abnormalities. A number of these malformations are depicted in Figs 1*C* and *D*, 2*A–C* and 3. The deformities were of varying complexity and were not evident in any of the fibres isolated from phenotypically normal (+/?) mice. A number of the dystrophic fibres were elongate but displayed a complex branching at their ends (Fig. 1*C*). Such branching may indicate a complex association of these fibres with their tendon insertions, although occasionally such a complexity was noted at a point along the fibre's length rather than at the fibre ends. Other fibres, which appeared to be of normal morphology under low magnification (×40), in fact had grooves along large portions of the fibre length which in some cases led to an internal cavity (Fig. 1*D*).

One of the most common fibre abnormalities was the presence of a single branch within the fibre, usually of unequal diameter (Fig. 2*A*) with the main body of the fibre. Another common abnormality was a simple combination of a larger number of single-bodied branches as is depicted in Figs 2*B* and 3*A*. Less frequently complex interconnections of appendages of various sizes and shapes were apparent (Fig. 2*C*). The individual appendages ranged in size from as small as 2–3 $\mu$ in diameter to 50–60 $\mu$m and this resulted in large differences in the apparent diameter of the fibre segments (5–180 $\mu$m).

*What constitutes a single fibre?*

It was absolutely essential to determine the actual boundaries of a single functional fibre to establish whether these complex structures were not simply strong structural associations between more than one discrete cell. The most direct way to do this was to look for intracellular continuity between the various branches of a complex structure such as the fibre shown in Fig. 3*A*. A higher magnification view of a small area of this structure is displayed in Fig. 3*B*. This shows an apparent bridge or cross-link between two of the main branches of the fibre, and indicates that there is a continuity of a sarcomere pattern through the bridge between branches. The structure could not be mechanically divided at this point, and other appendages

Fig. 1. Representative morphology of murine skeletal muscle fibres isolated by enzymatic dissociation. *A*, a soleus muscle fibre from a phenotypically normal (+/?) mouse. *B*, an apparently normal FDB muscle fibre from a dystrophic (dy/dy) animal. *C* and *D*, various morphological abnormalities found in soleus (*C*) and EDL (*D*) fibres from muscles of dystrophic (dy/dy) animals. Scale bar: *A*, 400 $\mu$m; *B* and *C*, 100 $\mu$m; *D*, 55 $\mu$m.

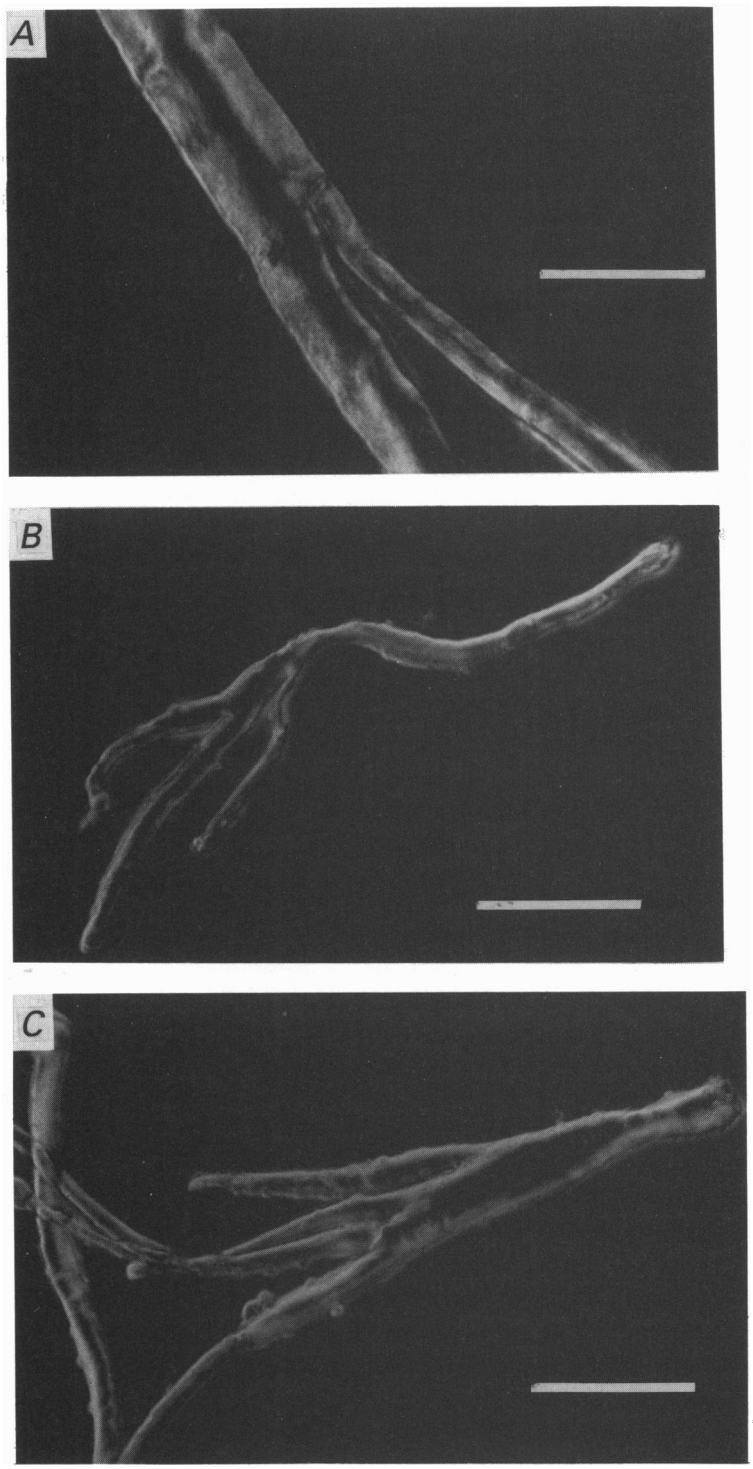


Fig. 2. For legend see facing page.

could not be simply removed from the main body of the fibre, without causing irreversible damage to the whole structure. This strongly suggested that the branches were not simply permanent associations between more than one fibre. Any attempt at locally damaging an individual appendage in the presence of normal Tyrode solution [$Ca^{2+}$] (1–2·5 mM) caused supercontraction of the total complex structure.

Intracellular continuity between the main body of the fibres and various appendages was also assessed by a number of physiological techniques. The fluorescent dye, Lucifer Yellow (lithium salt), was ionophoresed into the intracellular environment of fibres ($n = 9$) of varying complexity at a single focal point. As is apparent in Fig. 4, Lucifer Yellow was able to diffuse from the point of injection to occupy the cytoplasm of all appendages of deformed fibres indicating that no barrier existed, at any junction within the fibre, to the internal diffusion of this dye.

It was also possible to measure the resting membrane potential with an intracellular microelectrode at a number of locations in branches of deformed fibres. All values recorded from individual segments of a single, complex fibre were within a few millivolts of each others and two examples of five fibres tested are illustrated in Fig. 5. Fibre depolarization, which was initiated with the impalement electrode, always lead to the contraction of all branches which constituted part of a single fibre. It was apparent, however, that the contraction of individual branches within a single fibre (as detected by video frame-by-frame analysis, see Methods), was often unsynchronized, with some branches distal to the impalement electrode shortening before proximal branches.

*Contractile properties of chemically skinned segments from isolated muscle fibres*

The isolation of large numbers of intact, viable fibres from dystrophic animals allowed us to compare the $Ca^{2+}$ and $Sr^{2+}$ activation properties of the contractile apparatus, not only of different fibres, but also of the different parts of branched fibres chemically skinned with Triton X-100.

In Table 1 the results obtained with fibre segments from forty-four soleus fibres and twenty-seven EDL fibres are summarized. The following parameters were analysed: $pCa_{10}$, $pSr_{10}$ representing the $Ca^{2+}$ and $Sr^{2+}$ threshold for contraction; $pCa_{50}$, $pSr_{50}$ representing the sensitivity of the contractile apparatus for $Ca^{2+}$ and $Sr^{2+}$ respectively and the Hill coefficients $n_{Ca}$, $n_{Sr}$ which are associated with the steepness of the $Ca^{2+}$ and $Sr^{2+}$ activation curves respectively (Fink *et al.* 1986).

The activation characteristics of fibre segments from malformed EDL fibres were indistinguishable from those of fibre segments from fibres of normal appearance and both normal and malformed fibres displayed activation parameters which are very similar to those obtained in an earlier study with mechanically skinned fibre preparation from the same animal (Fink *et al.* 1986).

The soleus muscle of dystrophic mice which also contained both normal and

Fig. 2. Examples of the morphological abnormalities found in soleus muscle fibres from dystrophic dy/dy mice. *A*, a fibre branches into two parts of unequal diameter. *B*, a syncitium with three components. *C*, a fibre of extraordinary complexity, all parts shown were interconnected. Scale bar: *A*, 50 μm; *B* and *C*, 100 μm.

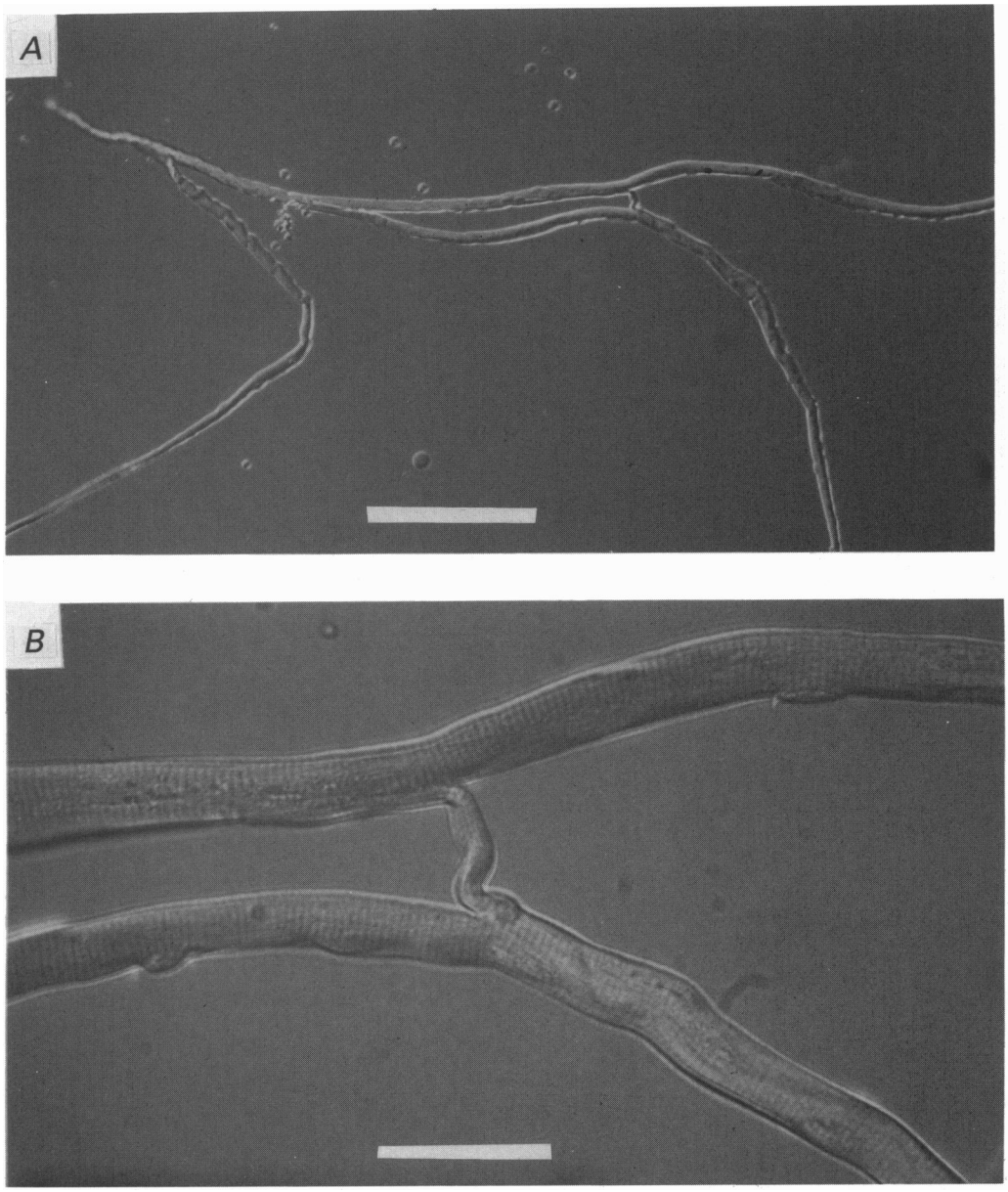


Fig. 3. *A*, a soleus fibre from a dystrophic (dy/dy) mouse which is composed of three large components of approximately equal size. *B*, a magnified view of *A* showing the small fibre segment which connects two components of the syncitium. Note the striation pattern in the connecting segment. Scale bar: *A*, 200 $\mu$m; *B*, 50 $\mu$m.

deformed fibres could be divided into two populations of fibres based on activation characteristics. The first population, which comprised more than 80% of the entire soleus fibres was characteristic of the single group of fibres previously identified in the soleus muscle of the same dystrophic animals (Fink *et al.* 1986). In this study we

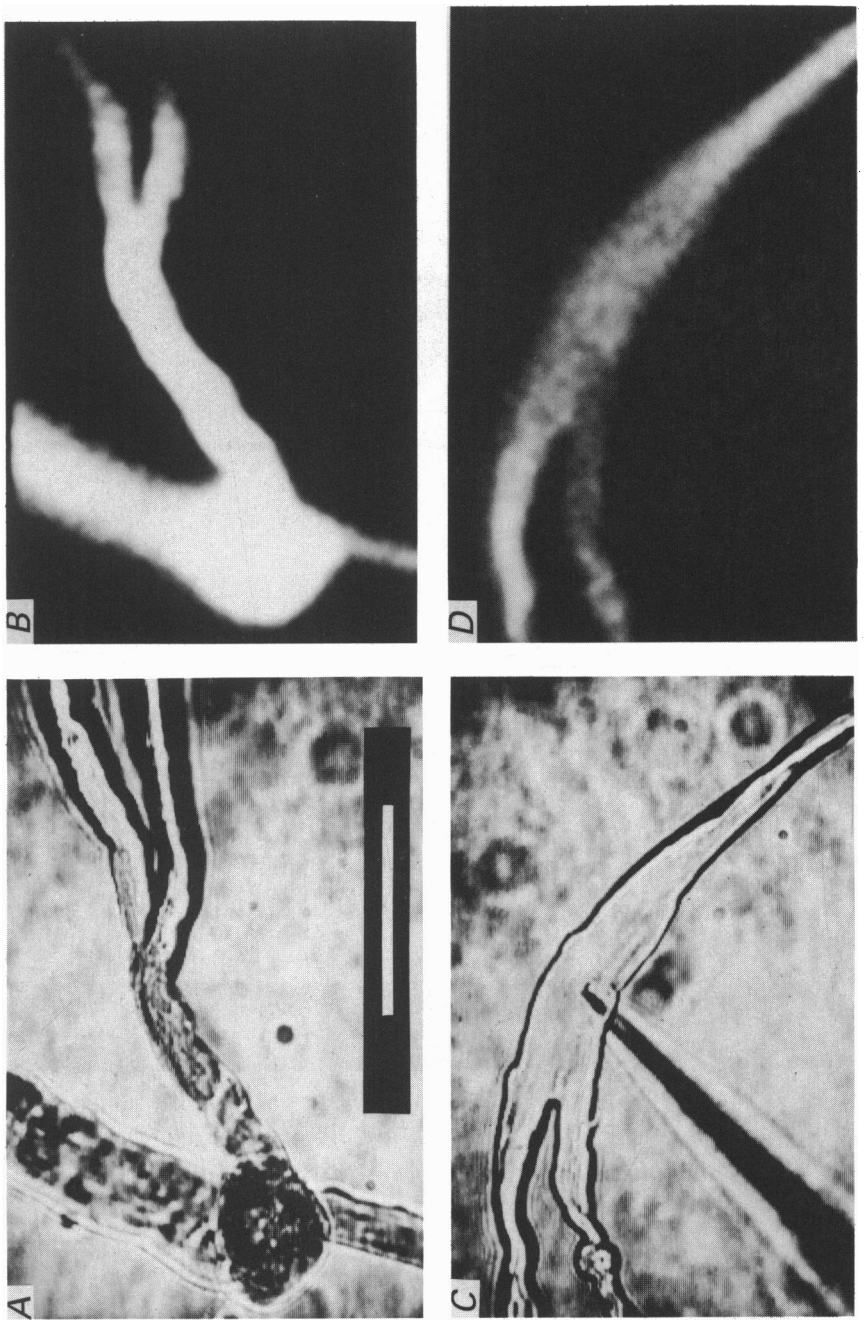


Fig. 4. Fluorescence images (*B* and *D*) of single intact dystrophic soleus muscle fibres with obvious morphological deformities (*A* and *C*) injected with Lucifer Yellow. The fluorescence images were frame averaged (four frames), corrected for illumination inhomogeneities and then contrast enhanced. The place of injection was located above the branching point of the fibre in (*A*) and in the centre of the fibre in (*B*) as shown by the shadow of the microelectrode. Scale bar in white on black background in $A = 80\ \mu m$ and is applicable to all panels. Resting membrane potentials: *A* and *B*, −63 mV; *C* and *D*, −60 mV.

could identify a second fibre population which differed from the first particularly with respect to its sensitivity to $Sr^{2+}$ which was one order of magnitude lower. The activation properties of this second fibre population resembles those of fast-twitch fibres from the soleus muscle of normal mice (Fink *et al.* 1986). For the contractile

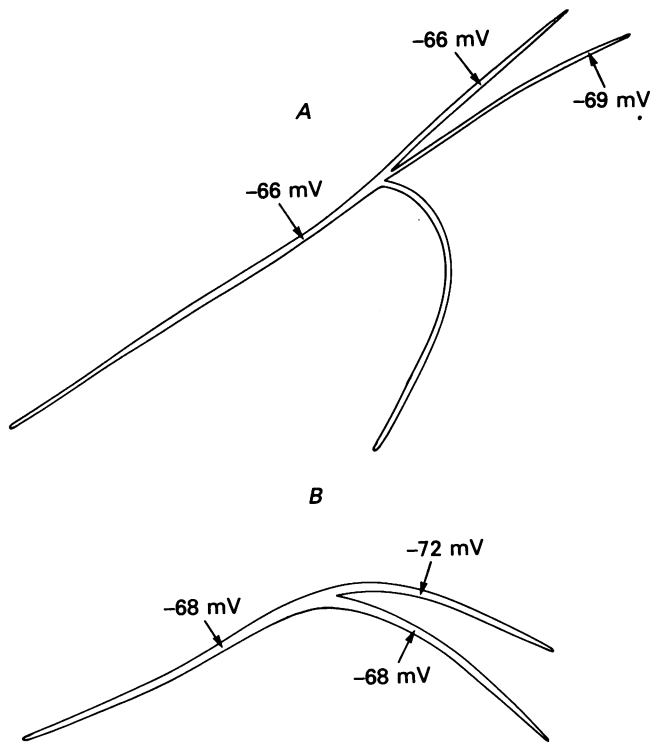


Fig. 5. Diagrammatic representations of two (*A* and *B*) malformed dystrophic (dy/dy) soleus muscle fibres showing the membrane potentials measured with 3 M-KCl-filled microelectrodes at different points of the syncitia.

characteristics listed in Table 1 there is no quantitative difference either within the EDL fibres, population 1 soleus fibres or population 2 soleus fibres between the malformed dy/dy fibres and dy/dy fibres of normal appearance. Fibres with fast-twitch characteristics (population 2) were found at a higher incidence among fibres of normal appearance, five out of twenty, than among deformed fibres, three out of twenty-four. The incidence of population 2 fibres in dy/dy soleus muscle is close to 18%, assuming that 56% (Table 1) of the total dystrophic soleus muscle fibres are malformed.

We were able to record complete contractile characteristics from at least two different segments of each of five complex fibre syncitia (two from the EDL and three from the soleus muscle). In all instances similar contractile characteristics were recorded in each branch of a syncitium. Figure 6 illustrates the isometric force–pCa and force–pSr from two segments of a malformed soleus fibre (inset of Fig. 6) both of which had fast twitch contractile properties characteristic of population 2 fibres (Table 1). As population 2 fibres occurred at low frequency in the soleus muscle (three out of twenty-four fibres) there would be a very low probability (0·016) of randomly

TABLE 1. $Ca^{2+}$ and $Sr^{2+}$ activation characteristics (mean ± S.E.M. ($n$)) of chemically skinned muscle fibres* from dystrophic mice (129 ReJ dy/dy)

| Muscle type | $pCa_{10}$ | $pCa_{50}$ | $n_{Ca}$ | $pSr_{10}$ | $pSr_{50}$ | $n_{Sr}$ | $pCa_{50}-pSr_{50}$ |
|---|---|---|---|---|---|---|---|
| EDL | | | | | | | |
| Fibres with deformities | 5·92 ± 0·04 (16) | 5·67 ± 0·06 (16) | 4·1 ± 0·3 (16) | 4·70 ± 0·02 (14) | 4·44 ± 0·02 (14) | 4·1 ± 0·3 (14) | 1·25 ± 0·05 (14) |
| Fibres of normal appearance† | 5·91 ± 0·03 (11) | 5·67 ± 0·05 (11) | 4·1 ± 0·04 (11) | 4·66 ± 0·03 (11) | 4·43 ± 0·03 (11) | 4·1 ± 0·4 (11) | 1·27 ± 0·04 (11) |
| All fibres | 5·91 ± 0·03 (27) | 5·67 ± 0·04 (27) | 4·1 ± 0·3 (27) | 4·68 ± 0·02 (25) | 4·44 ± 0·02 (25) | 4·1 ± 0·3 (25) | 1·26 ± 0·04 (25) |
| Soleus | | | | | | | |
| Population 1 | | | | | | | |
| Fibres with deformities | 6·35 ± 0·05 (21) | 6·06 ± 0·05 (21) | 3·5 ± 0·3 (21) | 5·93 ± 0·03 (21) | 5·65 ± 0·03 (21) | 3·9 ± 0·3 (21) | 0·41 ± 0·05 (21) |
| Fibres of normal appearance† | 6·29 ± 0·08 (15) | 5·97 ± 0·09 (15) | 3·0 ± 0·2 (15) | 5·89 ± 0·09 (13) | 5·58 ± 0·10 (13) | 3·7 ± 0·5 (13) | 0·41 ± 0·09 (13) |
| All fibres | 6·33 ± 0·04 (36) | 6·02 ± 0·05 (36) | 3·3 ± 0·2 (36) | 5·91 ± 0·04 (34) | 5·62 ± 0·04 (34) | 3·8 ± 0·3 (34) | 0·41 ± 0·05 (34) |
| Population 2 | | | | | | | |
| Fibres with deformities | 6·21 ± 0·02 (3) | 5·97 ± 0·04 (3) | 4·2 ± 0·8 (3) | 4·90 ± 0·02 (3) | 4·59 ± 0·04 (3) | 3·3 ± 0·5 (3) | 1·37 ± 0·06 (3) |
| Fibres of normal appearance† | 6·25 ± 0·04 (5) | 6·05 ± 0·05 (5) | 4·9 ± 0·6 (5) | 5·06 ± 0·09 (5) | 4·80 ± 0·08 (5) | 3·6 ± 0·2 (5) | 1·26 ± 0·04 (5) |
| All fibres | 6·23 ± 0·07 (8) | 6·02 ± 0·04 (8) | 4·7 ± 0·5 (8) | 5·00 ± 0·06 (8) | 4·72 ± 0·06 (8) | 3·5 ± 0·2 (8) | 1·30 ± 0·03 (8) |

* When several segments from the same fibres were investigated, the average values were used for those fibres.

† As seen at 40× magnification.

selecting two consecutive fast-twitch fibres from the population of soleus muscle fibres, unless all parts of the syncitium have similar contractile activation properties. The fact that the other two syncitia from the soleus had slow-twitch contractile properties in all the different segments tested further supports the view that all parts of a syncitium have similar contractile activation characteristics.

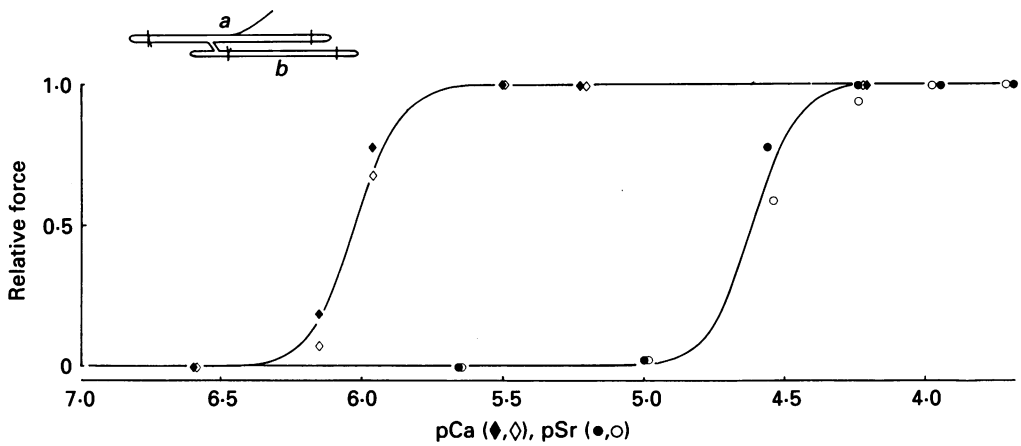


Fig. 6. The isometric force–pCa (◆, ◇) and force–pSr (●, ○) curves from two segments of a soleus malformed fibre (see diagrammatic representation in inset) which had contractile characteristics of population 2 (see Table 1). The open symbols refer to the results obtained with segment *a* and filled symbols to the results obtained with segment *b*. Dimensions of segments (diameter, length): *a*, 25 μm, 1·5 mm; *b*, 25 μm, 1·0 mm.

The majority of malformed fibres which were attached to the force transducer with a major morphological abnormality between the points of attachment broke upon maximal activation. When the same fibre was reclamped to exclude the deformed portion as depicted in Fig. 7 full isometric force–pCa and force–pSr curves were obtained showing that this soleus fibre was a typical slow-twitch fibre (population 1 in Table 1). This suggests that the breakage was entirely due to the mechanical weakness of the deformity and not due to an abnormality in the contractile proteins or in their regulatory mechanism in the straight segment of the fibre. This suggestion is further supported by the observation that when the cross-sectional area of the fibre either side of the deformity was similar, then the fibre could sustain maximal force without breaking (Fig. 6; segment *a*).

*Intact muscle properties*

Although it was obvious that individual fibres with morphological abnormalities were structurally weaker than fibres of normal morphology it did not necessarily follow that they would be at a functional disadvantage when embedded in the three-dimensional matrix of the intact muscle. To specifically investigate this question intact muscles from dystrophic animals were subjected to a rigorous protocol of repetitive, prolonged contractions for up to 3 h (see Methods) after which time they were allowed to recover from any fatigue-related reduction of force. Any resultant reduction in maximum tetanic force after this time when compared to unstimulated, contralateral muscles, or to muscles from phenotypically normal mice subjected to

the same stimulation protocol, was then recorded and taken as an indication of irreversible damage to some of the fibres within the muscle. With the aim of clarifying whether the malformed fibre syncitia could be affected by near-maximal isometric contractions of the intact muscle, all muscles were enzymatically

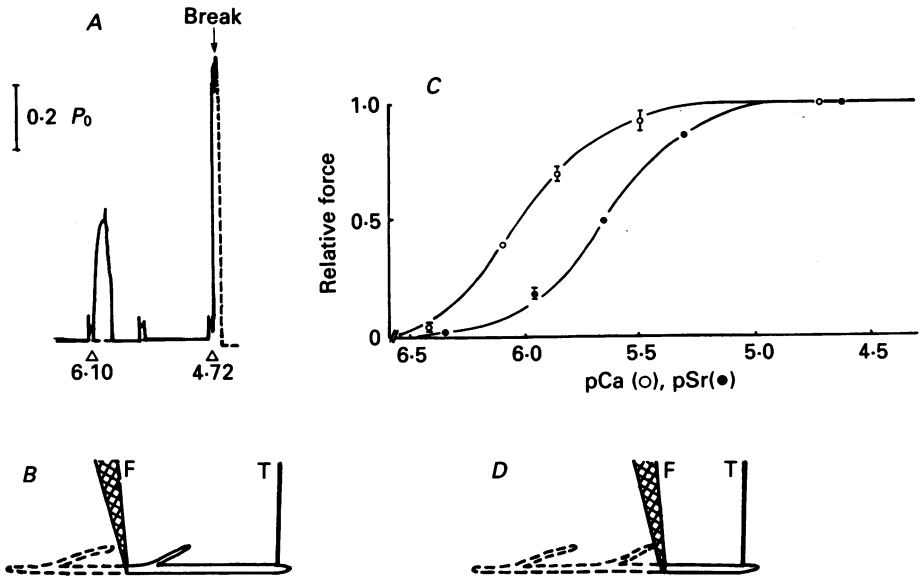


Fig. 7. Force activation by $Ca^{2+}$ and $Sr^{2+}$ of a fibre segment from a chemically skinned soleus fibre with deformities which broke when one of the deformities (schematically depicted in *B*) was present between the points of attachment of the fibre segment to the force measurement apparatus (forceps F and force transducer T). After breaking when about 75% maximum force ($P_0$) was reached (*A*), the segment of the fibre was relaxed and reattached to the force measuring system avoiding any deformity between the points of attachment (panel *D*). The force–pCa (○) and force–pSr (●) relations in this configuration are shown in *C*. The contractile characteristics of this fibre segment are those of fibre population 1 in Table 1. Fibre diameter, length and sarcomere length: *A* and *B*, 30 $\mu$m, 1·4 mm and 2·68 $\mu$m; *C* and *D*, 30 $\mu$m, 0·5 mm, 2·68 $\mu$m.

dissociated (as described in Methods) and the percentage of undamaged fibres possessing deformities of any sort (Figs 1*C* and *D*, 2 and 3) was compared to that of fibres with normal morphology (e.g. Fig. 1*B*). The results from the stimulated muscle were then compared with the unstimulated contralateral muscle to assess if there had been any decrease in the number of intact, malformed fibres present in the muscle as a result of the stimulation. The results of these experiments and the fibre population assessment are displayed in Table 2.

The stimulated muscles from dystrophic animals exhibited an irreversible decrease in the level of maximal tetanic force at the end of the stimulation protocol, of $35 \pm 2\%$ (mean $\pm$ S.D.) in soleus ($n = 3$ muscles), and 38% in one EDL muscle. No irreversible decrease in tetanic force was observed in experiments on either the soleus or the EDL muscles from phenotypically normal mice subjected to the same demanding stimulation protocol. There was also a marked reduction in the number of intact fibres with structural abnormalities in the stimulated dystrophic muscle, while the percentage of fibres with a normal appearance was concomitantly increased

as compared with the contralateral control muscles. It is therefore obvious that the morphologically abnormal fibres within the intact muscle were also not able to withstand maximal or near-maximal stimulation without undergoing irreversible damage, indicating that the intact dystrophic muscle is also at a functional disadvantage due to the presence of morphologically abnormal fibres.

TABLE 2. Percentage of intact* normal and intact* deformed muscle fibres in tetanically stimulated and control dystrophic soleus and EDL muscles

| Muscle type | Type of fibre | Unstimulated muscle (UM) (%) | Stimulated muscle (SM) (%) | Fibre population ratio (FPR) (SM/UM)† |
|---|---|---|---|---|
| Soleus (total fibres = 779) | Normal fibres | 44±8 ($n = 4$) | 79±4 ($n = 3$) | 1·52±0·25 ($n = 3$) |
| | Deformed fibres | 56±8 ($n = 4$) | 21±4 ($n = 3$) | 0·44±0·25 ($n = 3$) |
| EDL (total fibres = 428) | Normal fibres | 41±8 ($n = 4$) | 74±2 ($n = 2$) | 1·50±0·17 ($n = 2$) |
| | Deformed fibres | 59±8 ($n = 4$) | 26±2 ($n = 2$) | 0·51±0·17 ($n = 2$) |

* Fibres which are damaged supercontract and form part of the debris.

† Only contralateral pairs were used for this calculation. This ratio can be equated with the ratio between tetanic force at the beginning and at the end of the stimulation period after recovery (see text). Values are given as a percentage of the fibre type ± S.D. (number of muscles); all percentages are rounded to the nearest whole number.

## DISCUSSION

An enzymatic technique was developed which was successful in producing high yields of viable intact skeletal fibres from the muscles of phenotypically normal (+/?) and dystrophic (129/ReJ dy/dy) mice. This technique involved a single incubation phase in a collagenase mixture which was low in tryptic and protease activity (less than 0·03 and 27 units $mg^{-1}$ respectively). A similar protocol, but utilizing collagenase with high tryptic and protease activities (greater than 0·2 and 500 units $mg^{-1}$ respectively) has been used to liberate muscle fibres from the toe muscle of the laboratory rat (Bekoff & Betz, 1977). This difference may simply indicate a subtle connective tissue difference, or may be reflective of the large difference in muscle size between the two species. The dissociation in large numbers of single muscle fibres from dystrophic animals has enabled us to study the contractile properties of a much larger number of fibres than was previously possible with microdissection techniques (Fink *et al.* 1986). Thus, in the present study we could identify and characterize a new group of fibres with predominantly fast-twitch activation characteristics in the soleus muscle of dystrophic mice denoted, population 2 in Table 2, which occur with relatively low frequency (18%). These fibres are more sensitive to $Ca^{2+}$ by a factor of 1·7 and display steeper force–pCa curves (*t* test, $P < 0·02$) than the larger fast-twitch fibre population found in the soleus muscle of normal animals (Fink *et al.* 1986) but otherwise share similar characteristics with the latter fibre population. Moreover, the results strongly support the view expressed

earlier (Fink *et al.* 1986) that there are differences in the properties of the contractile and regulatory systems between normal and dystrophic murine fibres of the same type.

The majority of single fibres from the skeletal muscles of the dystrophic mouse show a myriad of structural abnormalities which are not present in fibres from the muscles of their normal counterparts (+/?). These abnormalities range from simple fibre splitting to tortuous interconnections of branches of vastly different diameters and lengths. There have been a limited number of reports that have suggested fibre splitting (Williams & Goldspink, 1976; Harris & Ribchester, 1979) and more complex muscle fibre structure in the same dystrophic animal model (Isaacs *et al.* 1973; Williams & Goldspink, 1976; Ontell & Feng, 1981). However, the extent of the abnormalities has never been visualized, and it has never previously been possible to isolate intact living fibres from the affected muscles to allow investigation of the functional and structural significance of these fibre abnormalities.

These abnormalities are extremely wide spread in dystrophic muscle. In a study of 129/ReJ dy/dy of approximately the same age (8–12 weeks) as used in this study, Isaacs *et al.* (1973) estimated that approximately 19% (twelve of sixty-four fibres) in a 1·5 mm length of gracilis muscle displayed branching which ranged from simple splits to complex fibre structures. This represents a gross underestimate, as many of the abnormal fibres probably were not detected with the techniques of serial section reconstruction. We have determined that the figure is likely to be much higher with up to 60% of the total fibre population displaying morphological abnormalities. The presence of a majority of deformed fibres within a muscle which possess multiple connected segments as demonstrated in this work (Figs 1*C* and *D*, 2 and 3) must call into question the estimate of the total fibre numbers obtained by counting the profile from a serial section through the muscle. Syncitia with three branches, e.g. Fig. 3*A*, would be counted as three distinct fibres by this method and as such the total fibre count obtained in this way would be a gross overestimate.

Importantly, we found that morphological abnormalities occur in fibres which show predominantly slow- or fast-twitch characteristics. Therefore, deformities are not restricted to fibres of a certain fibre type. There is no doubt that these complex structures actually represent functionally discrete single muscle fibres as we could show with a number of independent techniques.

Structural abnormalities have important functional implications for the affected muscle fibres. Asynchronous contractile activity is evident within branches of a single fibre in which there was large variation in the fibre diameter. Although there is a homogenous resting membrane potential at points on all branches within a fibre, the muscle action potential would be expected to be conducted more slowly along the narrow split bridges or the cross-links between fibres (as represented in Fig. 3*B*), because the diameter is a key factor in determining the speed of propagation of the action potential (Aidley, 1978). Such asynchrony in itself could lead to a large degree of muscle stretching with actively contracting regions pulling on less active or inactive regions, and if some parts of the fibre contracted and pulled on branches which were anchored to distant and independent sites then fibre damage could ensue. It is also likely that the sarcolemma is weak at the branch points of a syncitium making it a focal point for damage, $Ca^{2+}$ entry and loss of sarcoplasmic enzymes.

It is reasonable, given the results seen in Table 2, to assume that the irreversible

decrease in force seen in the stimulated dystrophic muscles is largely due to the selective damage of the malformed fibres. Therefore, we can predict (see Table 2) that there should be a decrease in the maximum force by a factor which represents the fractional force output of the damaged fibres. The normal fibre population (NF), which does not appear to be affected by the stimulation protocol can be used as a 'label' for the total (normal and deformed) number of intact fibres in the unstimulated and stimulated muscles. If TF and TF′ represent the total intact fibre population in the unstimulated and stimulated muscles respectively, then the percentages of normal fibres in unstimulated and stimulated muscles will be 100 NF/TF′ and therefore we can define a term 'fibre population ratio' (FPR) where

$$\mathrm{FPR} = (\mathrm{NF}/\mathrm{TF}')/(\mathrm{NF}/\mathrm{TF}) = (\mathrm{TF}/\mathrm{TF}').$$

Accordingly, the total number of intact fibres should have decreased in the stimulated soleus and EDL muscle to 65% (1/1·52, see Table 2) and 67% (1/1·50, see Table 2), respectively compared to the control muscles. If the average possible force developed by a fibre with a normal appearance is the same as that developed by a fibre with deformities but with the same average diameter, then one would predict that the tetanic force at the end of the stimulation period should have decreased by 35 and 33% in the soleus and EDL muscles, respectively. These values are remarkably close to those of 34% for soleus and 38% for EDL muscles measured experimentally (see Results).

From the results obtained in this study we suggest that the presence of the morphologically abnormal, weak fibres in the skeletal muscles from 129/ReJ dy/dy dystrophic mice explains why the animal loses muscle fibres as it ages. Due to the continued use of the muscle the weak points of the abnormal syncitia are stressed allowing $Ca^{2+}$ entry into the muscle and leakage of sarcoplasmic enzymes into the extracellular fluids resulting in fibre damage and eventual fibre death. It also explains the elevated $Ca^{2+}$ found in the dy/dy muscle fibres (Bakker, Head, Stephenson & Williams 1989). As morphologically abnormal fibres have been reported in the most common human dystrophy, Duchenne muscular dystrophy (Isaacs *et al.* 1973), it is an exciting possibility that the weakness of these malformed fibres may explain some of the clinical symptoms of the disease; muscle weakness, progressive loss of muscle tissue and the presence of sarcoplasmic enzymes in the extracellular fluids, symptoms which are shared by the 129/ReJ dy/dy dystrophic mice.

This work was supported by grants from the NH&MRC and ARGS. We acknowledge the expert technical assistance of Ruth I. Cafarella.

## REFERENCES

AIDLEY, D. J. (1978). *The Physiology of Excitable Cells*, 2nd edn, Cambridge University Press, Cambridge.

BAKKER, A. J., HEAD, S. I., STEPHENSON, D. G. & WILLIAMS, D. A. (1989). Calcium levels in skeletal muscle fibres from phenotypically normal and dystrophic mice (129/ReJ +/?, dy/dy). *Journal of Physiology* **412**, 51*P*.

BEKOFF, A. & BETZ, W. (1977). Physiological properties of dissociated muscle fibres obtained from innervated and denervated adult rat muscle. *Journal of Physiology* **271**, 25–40.

FINK, R. H., STEPHENSON, D. G. & WILLIAMS, D. A. (1986). Calcium and strontium activation of skinned muscle fibres of normal and dystrophic mice. *Journal of Physiology* **373**, 513–525.

HARRIS, J. B. & RIBCHESTER, R. R. (1979). In *Muscular Dystrophy and Other Inherited Diseases of Skeletal Muscle in Animals*, ed. HARRIS, J. B. *Annals of the New York Academy of Sciences* **317**, 153–170.

HEAD, S. I., WILLIAMS, D. A. & STEPHENSON, D. G. (1988). Gross structural abnormalities of skeletal muscle fibres isolated from the dystrophic mouse (129ReJ, dy/dy). *Proceedings of the Australian Physiological and Pharmacological Society* **19**, 126*P*.

ISAACS, D. R., BRADLEY, W. G. & HENDERSON, G. (1973). Longitudinal fibre splitting in muscular dystrophy: a serial cinematographic study. *Journal of Neurology, Neurosurgery and Psychiatry* **36**, 813–819.

ONTELL, M. & FENG, K. C. (1981). The three-dimensional cytoarchitecture and pattern of motor innervation of branched striated myotubes. *Anatomical Record* **200**, 11–31.

ONTELL, M., HUGHES, D. & BOURKE, D. (1982). Secondary myogenesis of normal muscle produces abnormal myotubes. *Anatomical Record* **204**, 199–207.

ROWLAND, L. P. (1985). Clinical perspective: Phenotypic expression in muscular dystrophy. *Advances in Experimental and Medical Biology* **182**, 3–13.

STEPHENSON, D. G. & WILLIAMS, D. A. (1981). Calcium-activated force responses in fast- and slow-twitch skinned muscle fibres of the rat at different temperatures. *Journal of Physiology* **317**, 281–302.

STEWART, W. W. (1981). Lucifer dyes – highly fluorescent dyes for biological tracing. *Nature* **292**, 17–21.

WEBSTER, C., SILBERSTEIN, L., HAYS, A. P. & BLAU, H. M. (1988). Fast muscle fibers are preferentially affected in Duchenne Muscular Dystrophy. *Cell* **52**, 503–513.

WILLIAMS, D. A., HEAD, S. I., STEPHENSON, G. M. & STEPHENSON, D. G. (1988). Characteristics of enzymatically isolated skeletal muscle fibres with structural abnormalities from dystrophic mice. *Proceedings of the Australian Physiological and Pharmacological Society* **19**, 127*P*.

WILLIAMS, P. E. & GOLDSPINK, G. (1976). The effect of denervation and dystrophy on the adaptation of sarcomere number of the functional length of the muscle of young and adult mice. *Journal of Anatomy* **122**, 455–465.